Chapter 3

Synthesis & Characterization of CuONPs from different sources & evaluation of their anti-oxidant property

INTRODUCTION:

Nanotechnology is the combinational field of chemistry, biology, physics and engineering (Farokhzad and Langer, 2009; Ferrari,M. 2005; Fox, JL. 2000; Jiang et al. 2007; Peppas, NA. 2004; Sinha et al., 2006; Uchegbu, IF. 2006). The general definition which refers to the size of nanoparticles must be in the range of 1-100nm in one dimension at least. Generally top down and bottom up processes have been used for the synthesis of nanoparticles. Nanoparticles have unique physico-chemical property that confers the anticancer property of nanoparticles. In the field of oncology nanoparticles help in detection, imaging, treatment and prevention of the disease. Several reports of anticancer activity of bare nanoparticles and surface coated nanoparticles have been found (Bondarenko et al., 2013; Chen et al., 2009; Wang et al., 2015; Sankar et al., 2014).

Inorganic nanocrystalline metal oxides are more appropriate for biological application due to extremely high surface areas (Stoimenov et al., 2002). Copper based nanoparticles have been chosen in the current study due to its interesting electronic arrangement that radially helps in oxidation, reduction and provide chemical and thermal stability. On the other hand copper act as a cofactor in redox reaction and it is very cost effective and easily available (Pramanik et al., 2016). Copper oxide (CuO) which is a p-type semiconductor with band gap energy of 1.2 eV (Dipankar and Murugan, 2012; Udayabhanu et al., 2015). It has high catalytic reusability and has longer shelf life compared to organic and microbial agents (Das et al., 2013). Metal based nanoparticles can be synthesized by chemical and green method. Synthesis by chemical method including several toxic chemical can indiscriminately damage the cancer cells as well as normal cells. But in green synthesis no toxic chemicals are used. In this research plant leaves have been used for the stabilization of the nanoparticles. Carbohydrates, flavonoids, saponins, proteins, amino acids and terpenoids these phytochemicals are major components of plant extract. These components play a pivotal role in the synthesis of nanoparticles (Amooaghaie et al., 2015). For this reason green synthesized NPs are safer than chemical one. To evaluate the difference in toxicity, both chemical and green nanoparticles were synthesized and tested in this study. The pharmacological activities of both chemical and green nanoparticles on their effect as antioxidants were determined.

3. MATERIALS AND METHODS:

3.1. Chemicals:

Titron X-100, Tris–HCl, Tris buffer, Methanol, 2-benzoyl pyridine, sodium dicyanamide, Potassium Bromide, Sodium nitroprusside, Copper Sulphate, Sodium dodecyl sulphate (SDS), 2-vinylpyridine and all other chemicals were obtained from Merck Ltd and SRL Pvt. Ltd. Mumbai.

3.1.1. Synthesis of Copper oxide nanoparticles by chemical method:

A methanolic solution (5mL) of 2-benzoyl pyridine (0.366g; 2mmol) was added dropwise with constant stirring to a methanolic solution (10mL) of Copper (II) Sulphate pentahydrate (1mmol; 0.370g). The stirring was continued for further 0.5h and then an aqueous solution (5 mL) of sodium dicyanamide (0.178g; 2mmol) was added drop wise. After further 1h stirring, the resulting mixture was filtered and the filtrate was collected. Single crystals suitable for X-ray data collection were obtained from the filtrate after a few days (Yield: 87%). Then the solid compound are crushed well and heated at 620°C in a furnace for 2h. The black powder compound obtained was washed well in methanol and dried and used as chemical CuONPs (Adhikary et al., 2016).

3.1.2. Preparation of leaf extract:

Leaves of traditional plant *Azadirachta indica* (*A. indica*) were collected from the campus of the Vidyasagar University (22.4320° N, 87.2979° E), West Bengal, India. After 100gm of leaves of *A. indica* were taken and washed gently with double distilled water, the leaves were chopped and dried in a hot air oven. After the completion of the total drying process, these materials were pulverized in a grinder until fine dust and dissolved in distilled water(10g dust/100mL distilled water) followed by filtration with Whatman filter paper No.1. The filtrate was collected and freeze-dried and kept at 4^{o}C temperature for storage.

3.1.3. Synthesis of Copper oxide nanoparticles from green source (*A. indica*):

CuONPs were synthesized from a traditional medicinal plant *A. indica* in accordance with previous protocol (Sankar et al., 2014), with slight modifications. Analytical grade of cupric sulphate (5mM) 90 ml solution, prepared by de-ionised water was mixed with 20 ml of filtrate obtained previously in a magnetic stirrer at 60^{o} C temperature. The mixture was kept at room temperature. Gradually a brownish black precipitate was observed at the bottom of the conical flask. Then it was dried and kept in storage for further use as green synthesized CuONPs.

3.1.4. Characterization:

3.1.4.1. FT-IR spectroscopy of Chemical and green synthesized CuONPs:

To know the surface chemistry of NPs, FT-IR spectroscopy was carried out with a Perkin 118 Elmer FT-IR spectrometer (Spectrum Two FT-IR spectrometer, 119 Version: 10.03.07.01120) in compliance with Mohapatra et al. (2007).

3.1.4.2. Dynamic light Scattering and surface zeta potential:

The hydrodynamic sizes of NPs and zeta potential were measured by DLS (Dynamic Light Scattering) using a Zetasizer-Nano ZS (Malvern, Malvern Hills, U.K.) as previously described (Chattopadhyay et al., 2015). NPs of 100µg/mL concentration each were sonicated for 2min and two drops of aqueous suspension of NPs in millipore water was added to measure the size and surface zeta potential.

3.1.4.3. X-Ray Diffraction (XRD) Study of Chemical and green synthesized CuONPs:

X-ray powder diffraction study of NPs was done in solid state. Diffraction patterns were achieved using XPERT-PRO diffractometer (PANalytical Ltd., The Netherlands) according to the method of Das et al., (2017).

3.1.4.4. Scanning Electron Microscopic (SEM) image of Chemical and green CuONPs:

The surface morphology and particle size were analyzed by high resolution scanning electron microscopy (Hitachi S-3400N) (Chattopadhyay et al., 2013).

3.1.4.5. EDX study of Chemical and green synthesized CuONPs:

EDX study was performed to know the presence of elemental Cu along with other components. Analysis was done using JEOL JSM 6360 equipped with an EDX (energy dispersive X-ray) analyzer (Majumdar et al., 2013).

3.1.4.6. Transmission electron microscopic image of Chemical and green CuONPs:

The particle size and microstructure were studied by high resolution transmission electron microscopy in a JEOL 3010, Japan, operating at 200kV at a magnification of 100K(x) according to Das et al., (2017).

3.1.4.7. UV-visible spectroscopy of Chemical and green synthesized CuONPs:

UV-visible absorption spectra of Chemical and green synthesized CuONPs were analyzed by Shimadzu UV- 1800 spectrophotometer at room temperature (Das et al., 2017).

3.1.4.8. Ion dissolution study of Chemical and green synthesized CuONPs:

Chemical and Green synthesized CuONPs were suspended in a DMEM culture medium (without FBS and antibiotic). In Ion dissolution study, both NPs of highest concentrations (100µg/mL) were suspended in a DMEM media without FBS and antibiotic for 1 week at 37^{o}C. The supernatant thus obtained, was used to determine the free Cu ions in the medium through atomic absorption study (AAS) (Chattopadhyay et al., 2015). $CuSO_4$ was used as a standard at varied concentrations.

3.1.4.9. Antioxidant activity of chemically and green synthesized CuONPs:

The green CuONPs were synthesized using *A. indica* leaves extracts and chemical synthesis was done by chemical reaction and followed by heat decomposition method. After that, *in vitro* antioxidant activity of both the nanoparticles were estimated by DPPH assay, H2O2, nitric oxide and super oxide radical scavenging assays. Different concentration of CuONPs (1-100µg/ml) suspension was sonicated for 30 mins to avoid any agglomeration of NPs prior to the experiment. The absorbance was measured spectrophotometrically against the corresponding blank solutions (Kumar et al., 2012). The percentage of inhibition was evaluated using the following formula;

Radical scavenging activity (%) = O.D Control – O.D Sample/ O.D control X 100

3.1.4.10. 2, 2-diphenyl-1-picrylhydrazyl (DPPH) radical scavenging activity:

The free radical scavenging activities of chemical and green synthesized CuONPs were evaluated by DPPH assay. At first 200µl of DPPH solution were taken in a 96 well microtitreplate reader. Then 10µl of nanoparticles solution with different concentration (1µg/ml, 5µg/ml, 10µg/ml, 25µg/ml, 50µg/ml and 100µg/ml) and standards were added separately in the microtitreplate reader. The total mixture with different concentration in case of both nanoparticles were shaken and kept for 30 minutes at R.T. After that the spectrophotometer was used to measure the absorbance at 517nm (Huong et al., 1998).

3.1.4.11. Hydrogen Peroxide (H_2O_2) radical scavenging activity:

A solution of 20mM hydrogen peroxide was prepared in buffer (p^H 7.4). Different concentration (1-100 µg/ml) of test samples and standards were mixed with 2ml of hydrogen peroxide solution. At 230nm wavelength optical density was measured. Phosphate buffer without hydrogen peroxide was taken as a blank for the experiment (Jayaprakasha et al., 2004).

3.1.4.12. Nitric Oxide (NO) radical scavenging activity:

Griess-llosvoy reaction can detect nitrite ions which are produced by the interaction of nitric oxide with oxygen. This nitric oxide was produced by sodium nitroprusside in aqueous solution at neutral p^H. After adding sodium nitroprusside (2ml of 10mM) and 0.5ml PBS (1X) (p^H 7.4) to 0.5 ml of NPs suspension at different concentrations, the mixture was incubated for 150mins at room temperature. Subsequently, 0.5ml of the incubated mixture was added to 1.0ml sulfanilic acid reagent (33% sulfanilic acid in 20% glacial acetic acid), followed by incubation for 5min at room temperature. 30mins prior to the absorbance measurement, Naphthylenediaminedihydrochloride (0.1% w/v) was added and kept at room temperature (Sun and HO, 2005).

3.1.4.13. Superoxide Radical Scavenging Assay:

Non-enzymatic phenazinemethosulfate nicotinamide adenine dinucleotide (PMS-NADH) reacts with PMS, NADH and oxygen to produce Superoxide anions. The scavenging assay was estimated by the reduction of nitro blue (50µM) solution and 1ml of NADH (78µM) solution. 1ml of PMS (10µM) was added to the mixture to initiate the reaction (Kaur and Kapoor, 2002).

3.1.4.14. Gas Chromatography-Mass Spectroscopy (GC-MS) analyses:

GC-MS analysis of *A. indica* leaf extract was performed on a TRACE GC ULTRA GC System of Thermo Scientific fitted with a non-polar capillary column DB-5MS, coupled to POLARIS Q Mass Spectrometer.

The inert gas Helium (99.999%) was used as a carrier gas. The gas flow was maintained at a constant flow rate of 1.0mL/min. The injector and ion source temperatures were 240° C and 230º C respectively. The ionizing energy was 70 eV. Oven temperature was programmed. At first it was kept at 70° C (hold for 1min) to 280° C at a rate of 10°C/min. Methanol (1/100, v/v) was used to dilute the crude sample and filtered. The diluted leaf extracts (1µL) were taken in a syringe and injected into injector with a split ratio of 20:1. The diluted leaf extract must be free from any particulate matter. The technology used in POLARIS Q IS ION TRAP. The mass spectra were compared with NIST LIBRARY (U.S.A).

3.2. RESULTS:

3.2.1. FT-IR spectroscopy of Chemical and green synthesized CuONPs:

The FT-IR spectra of the green synthesized CuONPs showed the strectching vibrational frequencies of aliphatic and aromatic hydroxyl groups peak at around 3200-3400cm^{-1}(Fig. 3.2A). Similar result was observed by Yugandhar et al., 2017. The broadness of the peak is due to intermolecular hydrogen bonding among the hydroxyl group. The presence of aromatic ring at the range of 1600-1400cm^{-1} was also observed. Peak at 1632cm^{-1} corresponds to the stretching vibration of primary amines. The peak in the range of 450-530cm^{-1} corresponds to Cu-O metal oxygen vibration. The band in the range of 1030-1110cm^{-1} assigned C-O stretching vibrations, (Rehana et al., 2017) thereby explaining the assigned peak similar to the present study. 850-680cm^{-1} is due to aromatic C-H bending. From the FT-IR study of chemical CuONPs (Fig. 3.1A), metal-oxygen vibration and aromatic C-H stretching frequency were observed through characteristic peaks in the range of 483.68cm^{-1} and 752.78cm^{-1} respectively.

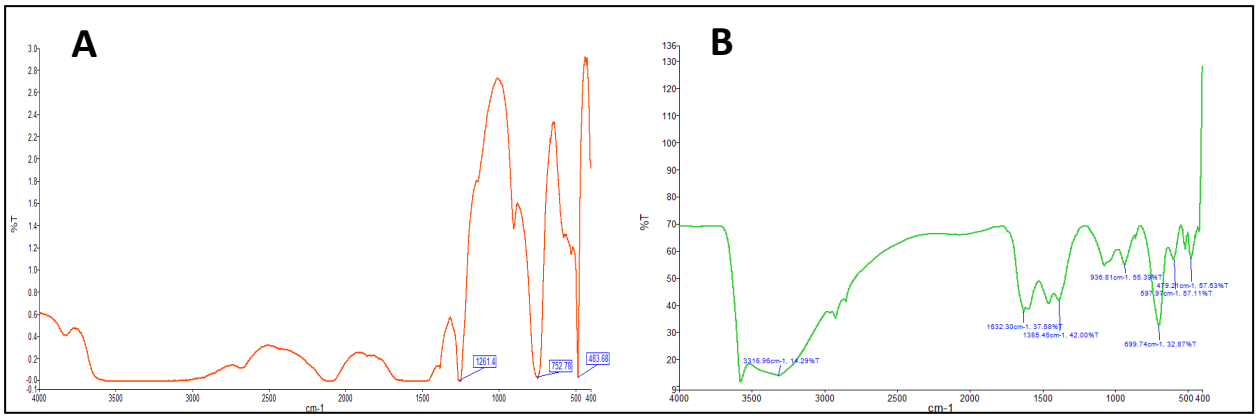

Fig.3.1: FT-IR spectra of **A)** Chemical CuONPs **B)** CuONPs from *A. indica*

3.2.2 Dynamic Light Scattering:

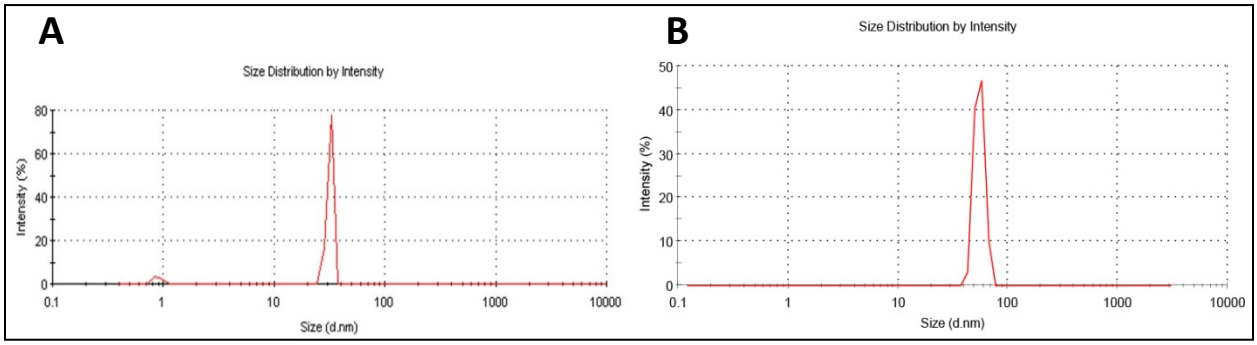

Figure 3.2: Hydrodynamic size measurement by DLS **A)** Chemical Copper oxide nanoparticles **B)** Copper oxide nano from *A. indica*

The mean hydrodynamic diameter (HD) of chemical CuONPs and Green synthesized CuONPs were 32.5±3nm (Fig.3.2A) and 55±10nm (Fig. 3.2.B).

3.2.3. Surface Zeta Potential of Chemical and green synthesized CuONPs:

The stability and agglomeration rate of Chemical CuONPs and green CuONPs were evaluated from the negative zeta potential (-18.35mv and -29.06mv) and polydispersity index (0.656 and 0.312) respectively.

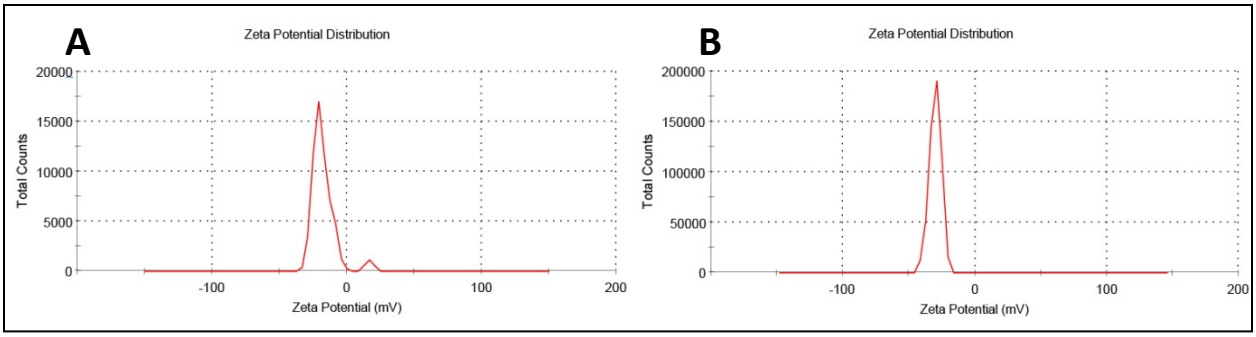

Figure 3.3: Surface zeta potential of **A)** Chemically synthesized CuONPs and **B)** Green synthesized CuONPs from *A. indica* leaves.

3.2.4. X-ray Diffraction study of Chemical and green synthesized CuONPs:

The purity and crystalline structure of chemical CuONPs and green CuONPs were measured by XRD pattern. XRD patterns of chemical CuONPs (Fig. 3.4A) showed noticeable peaks at 2θ values of 32^o, 35.64^o, 38.78^o,46^o, 53.5^o, 58.2^o, 66.24^o for the respectively marked indices of (110), (002), (111), (020), (113) respectively (Suresh et al., 2016). The XRD patterns of the green CuONPs (Fig. 3.4B) showed similar diffraction peaks without considerable shift in the peak position (Rehana et al., 2017). The spectrum demonstrated seven diffraction peaks at 2θ = 31.3, 35.5, 38.7, 48.7, 58.3, 61.5 and 66.2 can be perfectly attributed to the (110), (111), (200), (-202), (202), (-113) and (022) crystal planes, respectively. All the peaks of CuONPs were well matched with the diffraction pattern JCPDS No.05-0661. The well-defined CuO reflections in the observed PXRD patterns indicated the high crystallinity of both the synthesized nanoparticles. The synthesized CuONPs showed monoclinic crystalline structure of NPs. The broad band for the (111) and (200) reflections for the nanoparticle indicate that the size of the particles is in the nanometer range without any aggregation. The distinct CuO reflections observed in the XRD patterns indicates the high crystallinity of the synthesized green CuONPs.

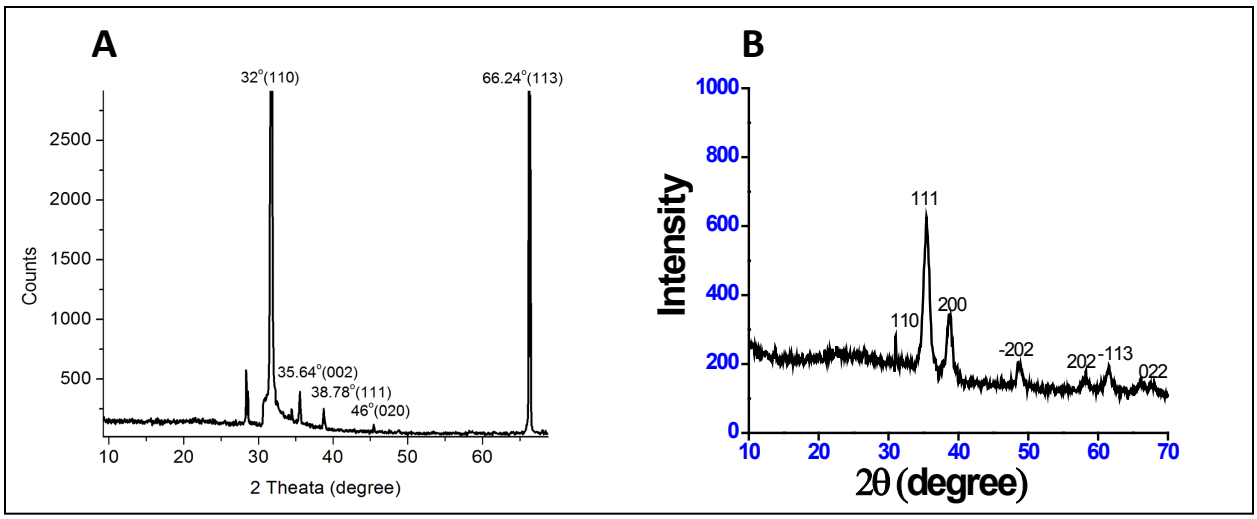

Figure 3.4: X-ray powder diffraction **A)** chemical CuONPs **B)** CuONPs from *A. indica*

3.2.5. Scanning Electron Microscopic image of Chemical and green synthesized CuONPs:

As shown in Fig.3.5A, chemically synthesized CuONPs exhibited rectangular shape with diameter 24±6nm, while green synthesized CuONPs showed spherical shape with diameter 44±9nm Fig.3.5.B.

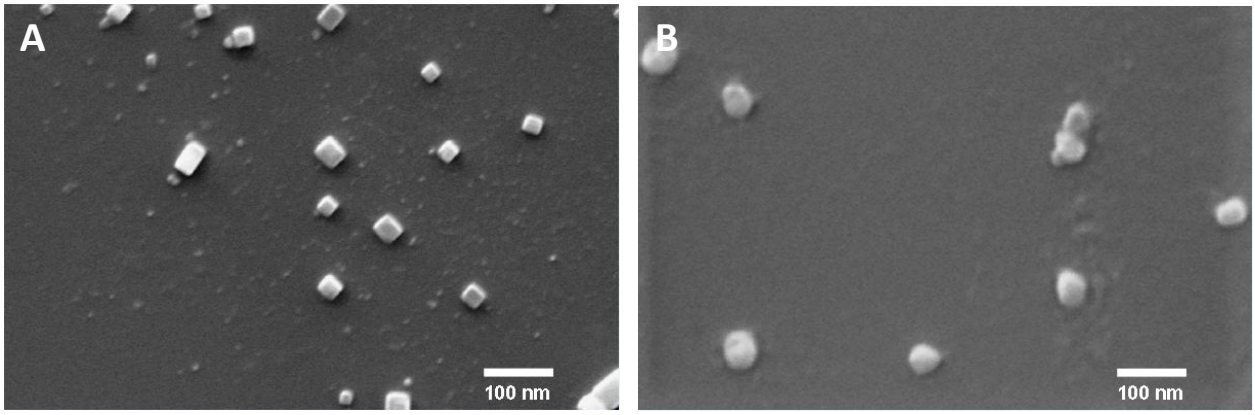

Figure 3.5: Scanning electron microscopic image of **A)** Chemical CuONPs **B)** CuONPs from *A. indica*

3.2.6. EDX study of Chemical and green synthesized CuONPs:

The purity and crystalline structure of chemical CuONPs and green CuONPs were measured by EDX. EDX of chemical CuONPs (Fig. 3.6A) showed elemental presence of Cu and Oxygen and the energy dispersive X-ray study in case of green CuONPs showed (Fig.3.6B) strong Cu signal

with other weak signals of oxygen, phosphorus and chlorine due to phenolic compounds, flavonoids, carbohydrates and saponin in the leaf extracts of *A. indica.*

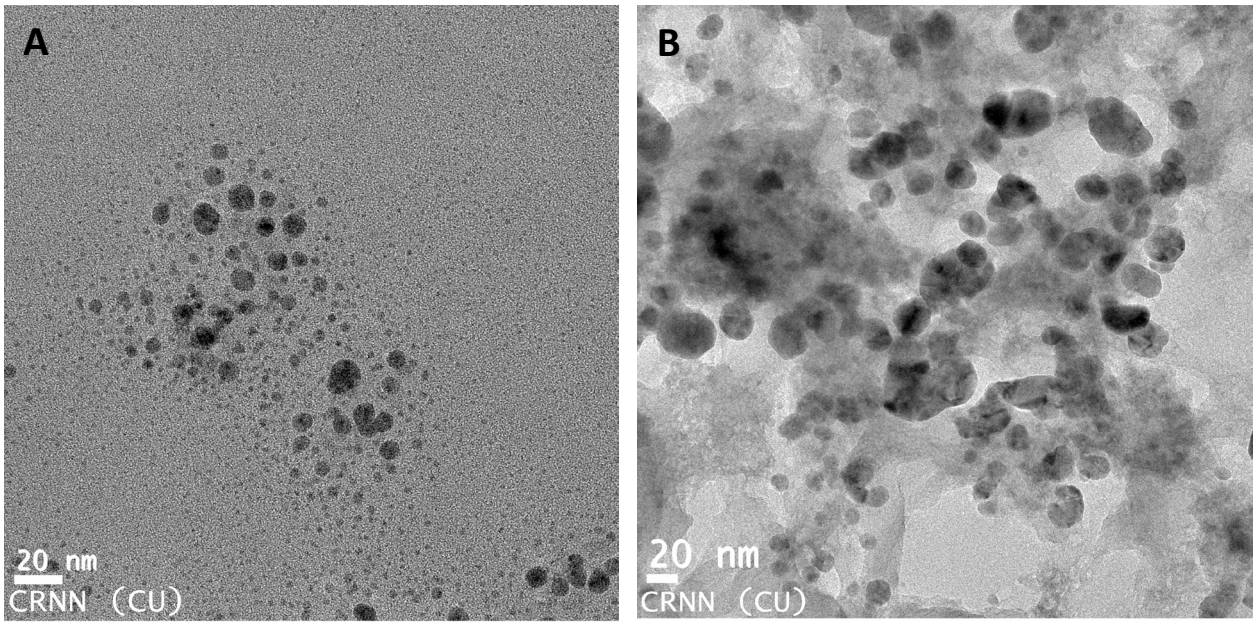

Fig. 3.7: Transmission electron microscopic image **A)** Chemical CuONPs **B)** CuONPs from *A. indica*

3.2.7. Transmission electron Microscopic image of Chemical and green synthesized CuONPs:

From the transmission electron microscopic image, the actual size of the nanoparticles was observed. The chemical CuONPs was 11.25±3nm in size and CuONPs from *A. indica* was 30.6±8nm in size.

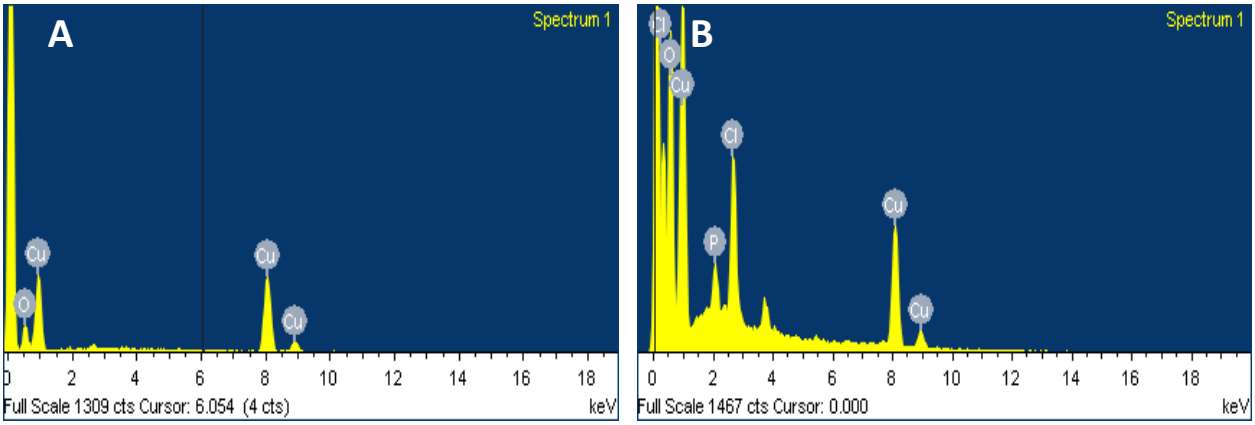

Figure3.6: EDX study of **A)** Chemical CuONPs **B)** CuONPs *from A. indica*

3.2.8. UV-Visible spectra of Chemical and green synthesized CuONPs:

Chemical and green synthesized CuONPs was successfully synthesized that was evident from UV-vis spectra. The chemically synthesized CuONPs showed the uv-visible peak at 282nm wavelengths and green synthesized CuONPs showed the uv-visible absorption peak at 293.2nm (Fig. 3.8).

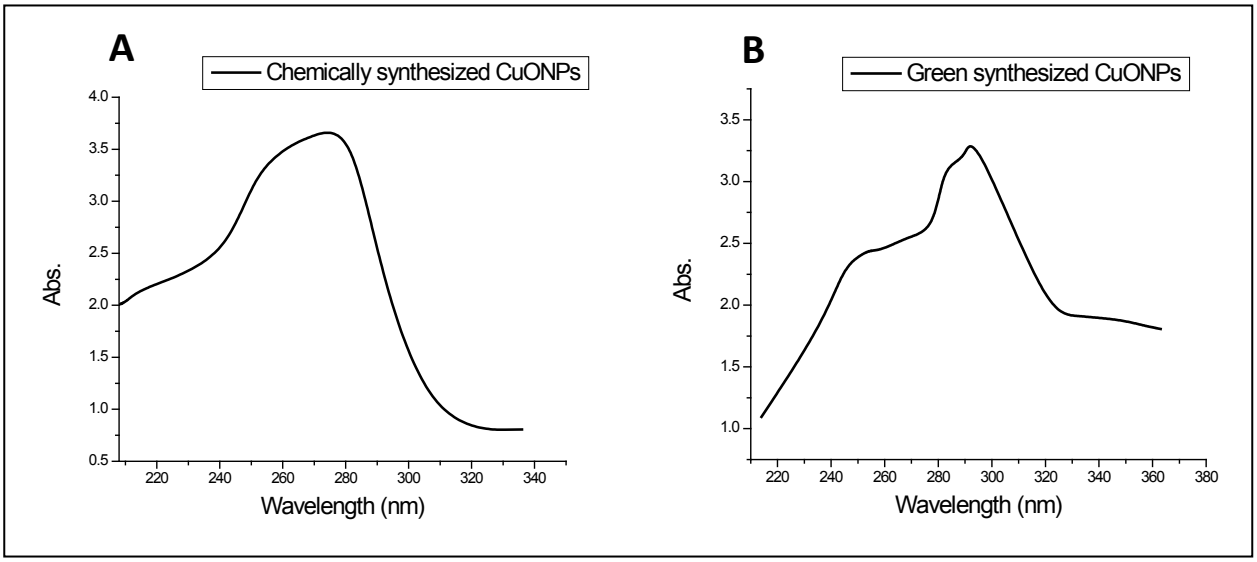

Figure 3.8: UV-Visible spectra of **A)** Chemically synthesized CuONPs and **B)** Green synthesized CuONPs

3.2.9. Ion dissolution study:

As shown in Fig. 3.9, Cu ions dissolution rates were 933PPM and 728PPM for chemically synthesized CuONPs and green synthesized CuONPs respectively at 100µg/mL dosage.

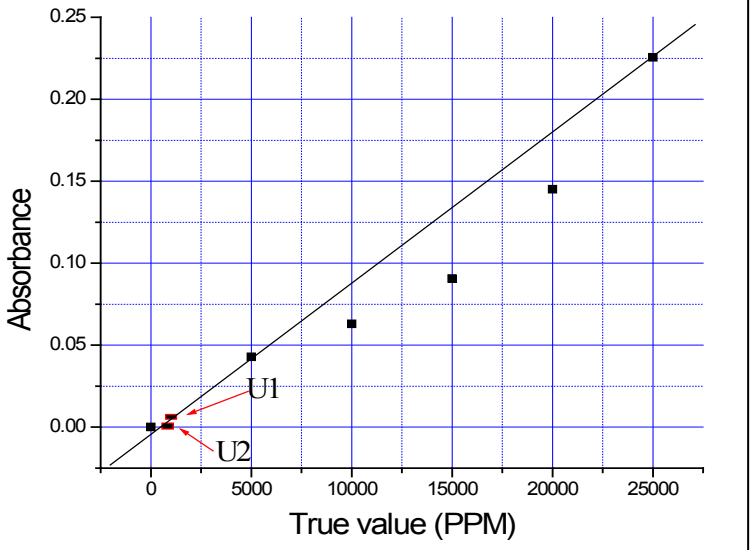

Figure 3.9: Ion dissolution study of Chemical CuONPs denoted as U1 and green CuONPs denoted as U2 in a FBS free medium.

3.3. Evaluation of anti-oxidant property of chemical & green CuONPs:

3.3.1. DPPH radical scavenging:

The chemically and green synthesized CuONPs both were able to reduce the DPPH radical (Fig.3.10A). As the dose increased gradually radical scavenging activity increased. The IC_{50} value for ascorbic acid, chemical CuONPs and green CuONPs were 21.35µg/ml, 55.40µg/ml and 28.95µg/ml (Fig 3.10B).

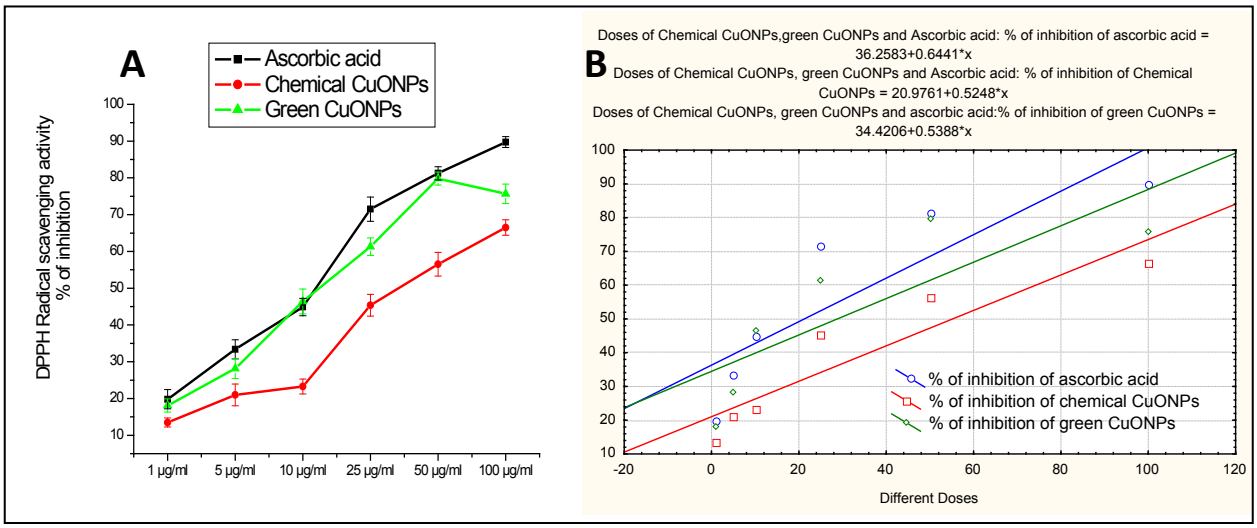

Figure 3.10: Pharmacological activities of chemical and green synthesized CuONPs. **(A)** DPPH radical scavenging activity **(B)** IC_{50} value of ascorbic acid, chemical and green synthesized CuONPs.

3.3.2. Hydrogen Peroxide radical scavenging:

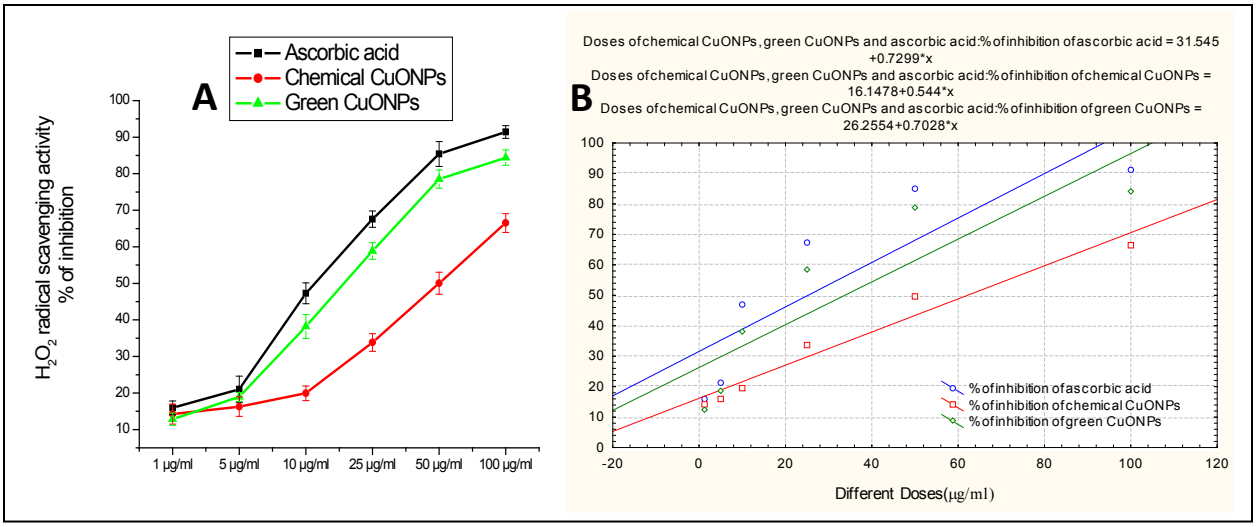

Figure 3.11: (A) H_2O_2 radical scavenging activity **(B)** IC_{50} value of ascorbic acid, chemical and green synthesized CuONPs.

H_2O_2 radical scavenging activity of green CuONPs was better than chemical one. The IC_{50} value for ascorbic acid, chemical CuONPs and green CuONPs were 25.32µg/ml, 62.24µg/ml and 33.83µg/ml respectively (Fig. 3.11B).

3.3.3. Nitric oxide scavenging:

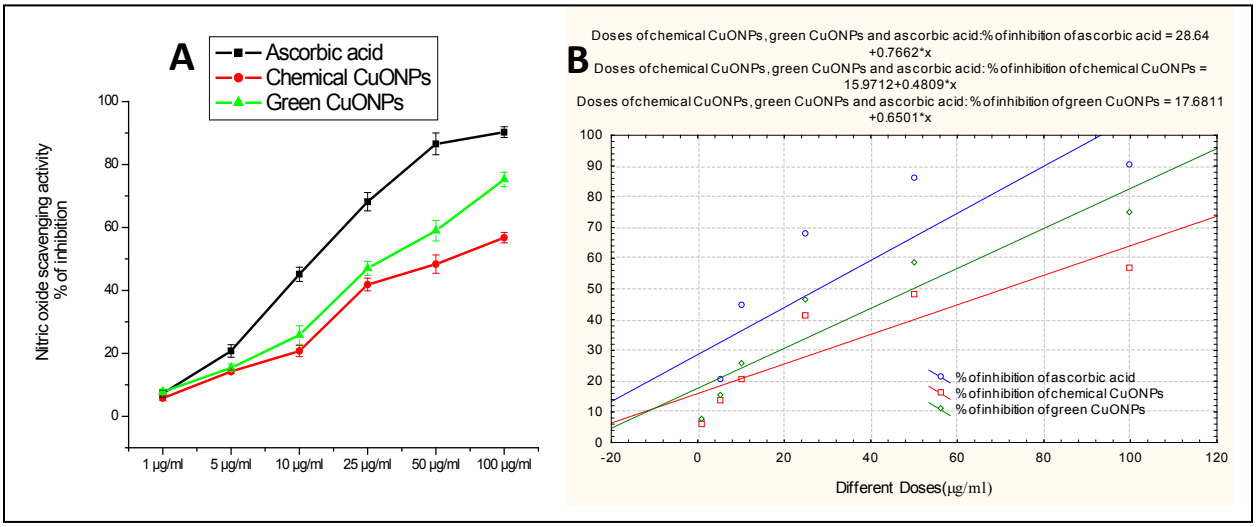

Figure 3.12: (A) Nitric Oxide radical scavenging activity. **(B)** IC_{50} value of ascorbic acid, chemical and green synthesized CuONPs.

Nitric oxide (NO) is an important chemical which is able to regulate several physiological processes. Generally it is generated by macrophages, neurons and endothelial cells. In the present

study, NO radical scavenging activity of chemical CuONPs and green CuONPs were elevated in a dose dependent manner (Fig 3.11A). Using the regression equation, the IC_{50} value for ascorbic acid, chemical CuONPs and green CuONPs were 27.88µg/ml, 70.89µg/ml and 49.72µg/ml respectively (Fig 3.12B).

3.3.4. Superoxide radical scavenging:

During the pathological events biomolecules of the system were damaged by OH-, peroxy nitrite or singlet oxygen those are generated by Superoxide anions. The superoxide anion radical scavenging activity was assayed by the PMS-NADH system and represented in Fig. 3.13A. Both the CuONPs were able to scavenge the superoxide anions in the system. The IC_{50} value for ascorbic acid, chemical CuONPs and green CuONPs were 34.94µg/ml, 68.32µg/ml and 44.99µg/ml respectively (Fig 3.13B).

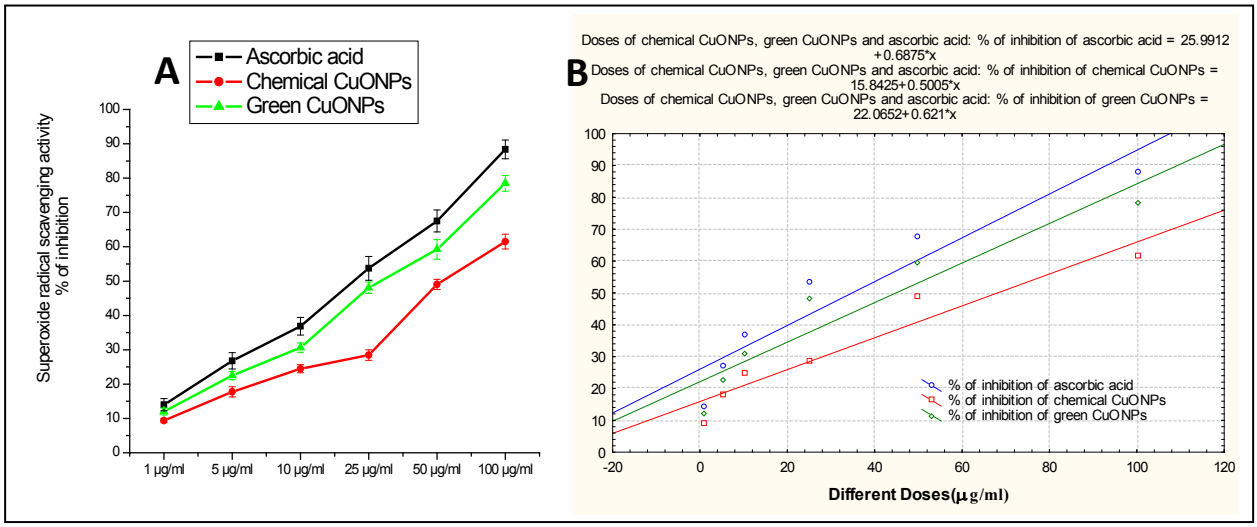

Figure 3.13: A) Superoxide radical scavenging activity. **(B)** IC_{50} value of ascorbic acid, chemical and green synthesized CuONPs.

3.3.5. Analysis of bioactive components of *A. indica* leaf by GC Mass spectroscopy:

From the % of peak area of compositions it can be concluded that among the 8 compounds, 3 compounds are mostly available in the extract. These are Cis-8,11,14-Eicosatrienoic Acid, Cis-5,8,11,14,17-Eicosapentaenoic acid and Retinoic acid. Cis-8,11,14-Eicosatrienoic Acid and Cis-5,8,11,14,17-Eicosapentaenoic acid both has pure omega-6 long-chain fatty acid methyl ester. Methyl ester has been considered as a standard for several biological studies. Dihomogamma-linolenic acid (DGLA) which is an essential omega-6 polyunsaturated fatty acid, possess

remarkable anti-inflammatory and anti-cancer activities (Wang et al., 2012) (Palakurthi et al.,

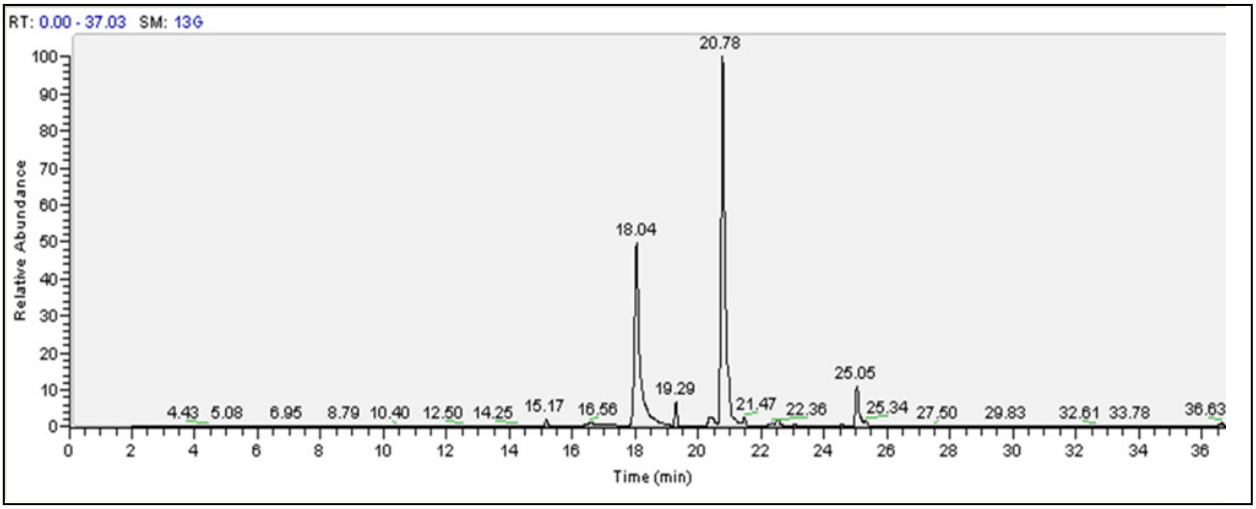

Figure 3.14: GC-MS chromatogram of water extract of leaf of *A. indica*.

2000). Retinoic acid is well known for its promising anticancer activity (Cristianoa et al., 2017).

Sl.No	Retention time	Compound	% of Area	MW	Molecular Formula
1.	16.56	2-Pentadecan-4-yne	1.69	206	C15H26
2.	17.17	Methyl 8-hydroxy-17-octadecene-9,11-diynoate	1.19	304	C19H28O3
3.	18.04	Cis-8,11,14-Eicosatrienoic Acid	29.1	306	C20H34O2
4.	19.29	Glycidyl Palmitate	1.88	312	C19H36O3
5.	20.37	9,12, 15 - Octadecatrien-1-ol	1.51	264	C18H32O
6.	20.78	Cis-5,8,11,14,17-Eicosapentaenoic acid	52.14	302	C20H30O2
7.	22.52	5,8,11- Heptadecatrien-1-ol	1.81	250	C17H30O
8.	25.05	Retinoic acid	5.78	300	C20H28O2

Table No.3.1: Bioactive components of water extract of *A. indica* leaf detected by GCMS analysis

3.4. DISCUSSION:

Both chemical and green CuONPs were synthesized by using two different methods. In the chemically synthesized process several chemicals were used and at last thermal decomposition was done at 620°C in a furnace for 2hr. But in case of green synthesized method leaves of *A. indica* were used. The water extract of leaves helps to stabilize the CuONPs. In both, the cases copper sulphate salt has been used as a precursor. Then both CuONPs were characterized by several physico-chemical techniques.

Water extracts of leaves contain several secondary metabolites like phenolic compounds, triterpinoids, flavonoids, alkaloids etc. which help in the stabilization process during the formation of nanoparticles from plant extracts (Aromal and Philip, 2012). These metabolites contain several multi-functional groups that induce an electrostatic double layer and protect the NPs from agglomeration, leading to stability of the NPs which can be explained by DLVO (Derjaguin-Landau-Verwey-Overbeek) theory (Missana and Adell, 2000). In compliance with DLVO theory, non-ionic part of the plant material will be coated on the surface of the NPs and inhibit the particle aggregation.

The characterizations of particles were done through FT-IR, DLS, XRD, EDX, SEM and TEM. Different bioactive flavonoid groups were found on metal surfaces through FT-IR (Sankar et al., 2014). Flavonoids contain various functional groups that are capable of NPs formation by actively chelating metal ions with their carbonyl group or pi electron. This mechanism helps to be absorbed these flavonoids onto the surface of nascent NPs which is defined as a nucleation stage of the NP.

The FT-IR study in case of green CuONPs showed the aromatic hydroxyl groups, phenolic OH and amine groups along with metal-oxygen vibration bond whereas chemical CuONPs showed the intense peak of metal oxygen vibrational bond without the presence of phenolic OH and any amines (Fig. 3.1). This result indicates the successful formation of CuONPs by both chemical and green method.

From DLS and SEM study it was confirmed that all CuONPs were in nano size range with different morphologies. The average particle size was in between 10 to 40 nm for all the NPs. SEM study conferred the morphology of the particles. Chemical CuONPs were rectangular in

shape whereas green CuONPs were spherical in shape (Fig. 3.5). Different shape and size affect the contribution of NPs in medicinal field (Lin et al., 2015). The negative surface zeta potential from DLS study indicated stability in both CuONPs. Chemical CuONPs showed -18.35mv and green CuONPs showed -29.06mv and polydispersity index (0.656 and 0.312) respectively. The highest negative value of surface zeta potential was observed in case of *A. indica* derived CuONPs, thus indicating greater stability. The disaggregation, favorable dispersity and stability of the particles may be attributed to the biofunctionalised groups present on the NP surfaces (Guerrini et al., 2018). Biologically active components present in plant plays a key role in the morphology of the nanoparticles (Makarov et al., 2014).

EDX study (Fig.3.6) validated the presence of Cu as a principal element while the FCC crystalline structure of CuONPs was confirmed by XRD study (Fig. 3.4). The presence of minute amounts of other particles namely Ca, P, O, Cl, Al and Zn may be attributed to the macromolecules like flavonoids, phenolic compounds, glyco-sides, carbohydrates, saponins present in the extracts (Zhang et al., 2009). EDX study also revealed the purity of the NPs. The XRD pattern of both the NPs clearly indicated the crystalline monoclinic structure of CuONPs not the CuNPs. The ion dissolution study conferred that the dissolution rate of chemically synthesized CuONPs was more than green synthesized CuONPs in a serum free media (Fig. 3.9). The toxicity of NPs is closely related to the ion dissolution rate of NPs. Ion dissolution of NPs depends upon the shape, size, composition and surface coating of the NPs (Lee et al., 2018). In the current study may be the surface coating with the bio-components inhibited the Cu ion release.

Enzymatic and non-enzymatic antioxidant substances regulate the free radical formation, which are linked to tumor formation. The free radical formation can be regulated by biomolecules like glycoprotein, proteins, fatty acids, lipids, phenolics, flavonoids and sugars (Marambio-Jones and Hoek, 2010). The radical scavenging power of antioxidants is worthwhile in managing cancer Moreover, the plant synthesized nanoparticles curbs the free radicals formation from the cell, thereby preventing cell proliferation and normal cell damage. Nanoparticles in moderate concentrations induce the apoptosis mechanism in malignant cells (Dipankar and Murugan, 2012).

The antioxidant properties of both CuONPs were evaluated. From the anti-oxidant profile through DPPH, H2O2 scavenging activity, NO radical scavenging activity and superoxide radical scavenging activity it was observed that the free radical scavenging activity of green CuONPs was better than chemical one compared to the ascorbic acid. This anti-oxidant property was attributed may be due to the bioactive components of *A. indica* water extract that were identified by GC mass spectroscopy (Fig. 3.14).

From the total study, it can be concluded that different shaped and sized NPs were successfully synthesized. After the successful synthesis and characterization, its free radical scavenging activity and anti-oxidant properties were evaluated. The free radical scavenging activity and as well as anti-oxidant property of green synthesized CuONPs was better than chemically synthesized CuONPs. So, the bioactive components of leaf extract which have been used to synthesize CuONPs may be contributing towards the enhanced medicinal property. The toxicity of these CuONPs was analyzed against normal cells in the next study.